

Measurement of $t\bar{t}$ Spin Correlation in $p\bar{p}$ Collisions Using the CDF II Detector at the Tevatron

T. Aaltonen,²¹ B. Álvarez González^{v,9} S. Amerio,⁴¹ D. Amidei,³² A. Anastassov,³⁶ A. Annovi,¹⁷ J. Antos,¹² G. Apollinari,¹⁵ J.A. Appel,¹⁵ A. Apresyan,⁴⁶ T. Arisawa,⁵⁶ A. Artikov,¹³ J. Asaadi,⁵¹ W. Ashmanskas,¹⁵ B. Auerbach,⁵⁹ A. Aurisano,⁵¹ F. Azfar,⁴⁰ W. Badgett,¹⁵ A. Barbaro-Galtieri,²⁶ V.E. Barnes,⁴⁶ B.A. Barnett,²³ P. Barria^{cc,44} P. Bartos,¹² M. Bauce^{aa,41} G. Bauer,³⁰ F. Bedeschi,⁴⁴ D. Beecher,²⁸ S. Behari,²³ G. Bellettini^{bb,44} J. Bellinger,⁵⁸ D. Benjamin,¹⁴ A. Beretvas,¹⁵ A. Bhatti,⁴⁸ M. Binkley^{*,15} D. Bisello^{aa,41} I. Bizjak^{gg,28} K.R. Bland,⁵ B. Blumenfeld,²³ A. Bocci,¹⁴ A. Bodek,⁴⁷ D. Bortoletto,⁴⁶ J. Boudreau,⁴⁵ A. Boveia,¹¹ B. Brau^{a,15} L. Brigliadori^{z,6} A. Brisuda,¹² C. Bromberg,³³ E. Brucken,²¹ M. Bucchiantonio^{bb,44} J. Budagov,¹³ H.S. Budd,⁴⁷ S. Budd,²² K. Burkett,¹⁵ G. Busetto^{aa,41} P. Bussey,¹⁹ A. Buzatu,³¹ C. Calancha,²⁹ S. Camarda,⁴ M. Campanelli,³³ M. Campbell,³² F. Canelli^{12,15} A. Canepa,⁴³ B. Carls,²² D. Carlsmith,⁵⁸ R. Carosi,⁴⁴ S. Carrillo^{k,16} S. Carron,¹⁵ B. Casal,⁹ M. Casarsa,¹⁵ A. Castro^{z,6} P. Catastini,¹⁵ D. Cauz,⁵² V. Cavaliere^{cc,44} M. Cavalli-Sforza,⁴ A. Cerri^{f,26} L. Cerrito^{q,28} Y.C. Chen,¹ M. Chertok,⁷ G. Chiarelli,⁴⁴ G. Chlachidze,¹⁵ F. Chlebana,¹⁵ K. Cho,²⁵ D. Chokheli,¹³ J.P. Chou,²⁰ W.H. Chung,⁵⁸ Y.S. Chung,⁴⁷ C.I. Ciobanu,⁴² M.A. Ciocci^{cc,44} A. Clark,¹⁸ G. Compostella^{aa,41} M.E. Convery,¹⁵ J. Conway,⁷ M. Corbo,⁴² M. Cordelli,¹⁷ C.A. Cox,⁷ D.J. Cox,⁷ F. Crescioli^{bb,44} C. Cuenca Almenar,⁵⁹ J. Cuevas^{v,9} R. Culbertson,¹⁵ D. Dagenhart,¹⁵ N. d'Ascenzo^{t,42} M. Datta,¹⁵ P. de Barbaro,⁴⁷ S. De Cecco,⁴⁹ G. De Lorenzo,⁴ M. Dell'Orso^{bb,44} C. Deluca,⁴ L. Demortier,⁴⁸ J. Deng^{c,14} M. Deninno,⁶ F. Devoto,²¹ M. d'Errico^{aa,41} A. Di Canto^{bb,44} B. Di Ruzza,⁴⁴ J.R. Dittmann,⁵ M. D'Onofrio,²⁷ S. Donati^{bb,44} P. Dong,¹⁵ M. Dorigo,⁵² T. Dorigo,⁴¹ K. Ebina,⁵⁶ A. Elagin,⁵¹ A. Eppig,³² R. Erbacher,⁷ D. Errede,²² S. Errede,²² N. Ershaidat^{y,42} R. Eusebi,⁵¹ H.C. Fang,²⁶ S. Farrington,⁴⁰ M. Feindt,²⁴ J.P. Fernandez,²⁹ C. Ferrazza^{dd,44} R. Field,¹⁶ G. Flanagan^{r,46} R. Forrest,⁷ M.J. Frank,⁵ M. Franklin,²⁰ J.C. Freeman,¹⁵ Y. Funakoshi,⁵⁶ I. Furic,¹⁶ M. Gallinaro,⁴⁸ J. Galyardt,¹⁰ J.E. Garcia,¹⁸ A.F. Garfinkel,⁴⁶ P. Garosi^{cc,44} H. Gerberich,²² E. Gerchtein,¹⁵ S. Giagu^{ee,49} V. Giakoumopoulou,³ P. Giannetti,⁴⁴ K. Gibson,⁴⁵ C.M. Ginsburg,¹⁵ N. Giokaris,³ P. Giromini,¹⁷ M. Giunta,⁴⁴ G. Giurgiu,²³ V. Glagolev,¹³ D. Glenzinski,¹⁵ M. Gold,³⁵ D. Goldin,⁵¹ N. Goldschmidt,¹⁶ A. Golossanov,¹⁵ G. Gomez,⁹ G. Gomez-Ceballos,³⁰ M. Goncharov,³⁰ O. González,²⁹ I. Gorelov,³⁵ A.T. Goshaw,¹⁴ K. Goulianos,⁴⁸ A. Gresele,⁴¹ S. Grinstein,⁴ C. Grosso-Pilcher,¹¹ R.C. Group,⁵⁵ J. Guimaraes da Costa,²⁰ Z. Gunay-Unalan,³³ C. Haber,²⁶ S.R. Hahn,¹⁵ E. Halkiadakis,⁵⁰ A. Hamaguchi,³⁹ J.Y. Han,⁴⁷ F. Happacher,¹⁷ K. Hara,⁵³ D. Hare,⁵⁰ M. Hare,⁵⁴ R.F. Harr,⁵⁷ K. Hatakeyama,⁵ C. Hays,⁴⁰ M. Heck,²⁴ J. Heinrich,⁴³ M. Herndon,⁵⁸ S. Hewamanage,⁵ D. Hidas,⁵⁰ A. Hocker,¹⁵ W. Hopkins^{g,15} D. Horn,²⁴ S. Hou,¹ R.E. Hughes,³⁷ M. Hurwitz,¹¹ U. Husemann,⁵⁹ N. Hussain,³¹ M. Hussein,³³ J. Huston,³³ G. Introzzi,⁴⁴ M. Iori^{ee,49} A. Ivanov^{o,7} E. James,¹⁵ D. Jang,¹⁰ B. Jayatilaka,¹⁴ E.J. Jeon,²⁵ M.K. Jha,⁶ S. Jindariani,¹⁵ W. Johnson,⁷ M. Jones,⁴⁶ K.K. Joo,²⁵ S.Y. Jun,¹⁰ T.R. Junk,¹⁵ T. Kamon,⁵¹ P.E. Karchin,⁵⁷ Y. Kato^{n,39} W. Ketchum,¹¹ J. Keung,⁴³ V. Khotilovich,⁵¹ B. Kilminster,¹⁵ D.H. Kim,²⁵ H.S. Kim,²⁵ H.W. Kim,²⁵ J.E. Kim,²⁵ M.J. Kim,¹⁷ S.B. Kim,²⁵ S.H. Kim,⁵³ Y.K. Kim,¹¹ N. Kimura,⁵⁶ M. Kirby,¹⁵ S. Klimenko,¹⁶ K. Kondo,⁵⁶ D.J. Kong,²⁵ J. Konigsberg,¹⁶ A.V. Kotwal,¹⁴ M. Kreps,²⁴ J. Kroll,⁴³ D. Krop,¹¹ N. Krumnack^{l,5} M. Kruse,¹⁴ V. Krutelyov^{d,51} T. Kuhr,²⁴ M. Kurata,⁵³ S. Kwang,¹¹ A.T. Laasanen,⁴⁶ S. Lami,⁴⁴ S. Lammel,¹⁵ M. Lancaster,²⁸ R.L. Lander,⁷ K. Lannon^{u,37} A. Lath,⁵⁰ G. Latino^{cc,44} I. Lazzizzera,⁴¹ T. LeCompte,² E. Lee,⁵¹ H.S. Lee,¹¹ J.S. Lee,²⁵ S.W. Lee^{w,51} S. Leo^{bb,44} S. Leone,⁴⁴ J.D. Lewis,¹⁵ C.-J. Lin,²⁶ J. Linacre,⁴⁰ M. Lindgren,¹⁵ E. Lipeles,⁴³ A. Lister,¹⁸ D.O. Litvintsev,¹⁵ C. Liu,⁴⁵ Q. Liu,⁴⁶ T. Liu,¹⁵ S. Lockwitz,⁵⁹ N.S. Lockyer,⁴³ A. Loginov,⁵⁹ D. Lucchesi^{aa,41} J. Lueck,²⁴ P. Lujan,²⁶ P. Lukens,¹⁵ G. Lungu,⁴⁸ J. Lys,²⁶

R. Lysak,¹² R. Madrak,¹⁵ K. Maeshima,¹⁵ K. Makhoul,³⁰ P. Maksimovic,²³ S. Malik,⁴⁸ G. Manca,^{b,27}
A. Manousakis-Katsikakis,³ F. Margaroli,⁴⁶ C. Marino,²⁴ M. Martínez,⁴ R. Martínez-Ballarín,²⁹
P. Mastrandrea,⁴⁹ M. Mathis,²³ M.E. Mattson,⁵⁷ P. Mazzanti,⁶ K.S. McFarland,⁴⁷ P. McIntyre,⁵¹
R. McNulty,^{i,27} A. Mehta,²⁷ P. Mehtala,²¹ A. Menzione,⁴⁴ C. Mesropian,⁴⁸ T. Miao,¹⁵
D. Mietlicki,³² A. Mitra,¹ H. Miyake,⁵³ S. Moed,²⁰ N. Moggi,⁶ M.N. Mondragon,^{k,15} C.S. Moon,²⁵
R. Moore,¹⁵ M.J. Morello,¹⁵ J. Morlock,²⁴ P. Movilla Fernandez,¹⁵ A. Mukherjee,¹⁵ Th. Muller,²⁴
P. Murat,¹⁵ M. Mussini,^{z,6} J. Nachtman,^{m,15} Y. Nagai,⁵³ J. Naganoma,⁵⁶ I. Nakano,³⁸ A. Napier,⁵⁴
J. Nett,⁵⁸ C. Neu,⁵⁵ M.S. Neubauer,²² J. Nielsen,^{e,26} L. Nodulman,² O. Norriella,²² E. Nurse,²⁸
L. Oakes,⁴⁰ S.H. Oh,¹⁴ Y.D. Oh,²⁵ I. Oksuzian,⁵⁵ T. Okusawa,³⁹ R. Orava,²¹ L. Ortolan,⁴
S. Pagan Griso,^{aa,41} C. Pagliarone,⁵² E. Palencia,^{f,9} V. Papadimitriou,¹⁵ A.A. Paramonov,²
J. Patrick,¹⁵ G. Pauletta,^{ff,52} M. Paulini,¹⁰ C. Paus,³⁰ D.E. Pellett,⁷ A. Penzo,⁵² T.J. Phillips,¹⁴
G. Piacentino,⁴⁴ E. Pianori,⁴³ J. Pilot,³⁷ K. Pitts,²² C. Plager,⁸ L. Pondrom,⁵⁸ K. Potamianos,⁴⁶
O. Poukhov,^{*,13} F. Prokoshin,^{x,13} A. Pronko,¹⁵ F. Ptohos,^{h,17} E. Pueschel,¹⁰ G. Punzi,^{bb,44}
J. Pursley,⁵⁸ A. Rahaman,⁴⁵ V. Ramakrishnan,⁵⁸ N. Ranjan,⁴⁶ I. Redondo,²⁹ P. Renton,⁴⁰
M. Rescigno,⁴⁹ F. Rimondi,^{z,6} L. Ristori,^{45,15} A. Robson,¹⁹ T. Rodrigo,⁹ T. Rodriguez,⁴³
E. Rogers,²² S. Rolli,⁵⁴ R. Roser,¹⁵ M. Rossi,⁵² F. Rubbo,¹⁵ F. Ruffini,^{cc,44} A. Ruiz,⁹ J. Russ,¹⁰
V. Rusu,¹⁵ A. Safonov,⁵¹ W.K. Sakumoto,⁴⁷ Y. Sakurai,⁵⁶ L. Santi,^{ff,52} L. Sartori,⁴⁴ K. Sato,⁵³
V. Saveliev,^{t,42} A. Savoy-Navarro,⁴² P. Schlabach,¹⁵ A. Schmidt,²⁴ E.E. Schmidt,¹⁵ M.P. Schmidt,^{*,59}
M. Schmitt,³⁶ T. Schwarz,⁷ L. Scodellaro,⁹ A. Scribano,^{cc,44} F. Scuri,⁴⁴ A. Sedov,⁴⁶ S. Seidel,³⁵
Y. Seiya,³⁹ A. Semenov,¹³ F. Sforza,^{bb,44} A. Sfyrla,²² S.Z. Shalhout,⁷ T. Shears,²⁷ P.F. Shepard,⁴⁵
M. Shimojima,^{s,53} S. Shiraishi,¹¹ M. Shochet,¹¹ I. Shreyber,³⁴ A. Simonenko,¹³ P. Sinervo,³¹
A. Sissakian,^{*,13} K. Sliwa,⁵⁴ J.R. Smith,⁷ F.D. Snider,¹⁵ A. Soha,¹⁵ S. Somalwar,⁵⁰ V. Sorin,⁴
P. Squillacioti,¹⁵ M. Stancari,¹⁵ M. Stanitzki,⁵⁹ R. St. Denis,¹⁹ B. Stelzer,³¹ O. Stelzer-Chilton,³¹
D. Stentz,³⁶ J. Strologas,³⁵ G.L. Strycker,³² Y. Sudo,⁵³ A. Sukhanov,¹⁶ I. Suslov,¹³ K. Takemasa,⁵³
Y. Takeuchi,⁵³ J. Tang,¹¹ M. Tecchio,³² P.K. Teng,¹ J. Thom,^{g,15} J. Thome,¹⁰ G.A. Thompson,²²
E. Thomson,⁴³ P. Ttito-Guzmán,²⁹ S. Tkaczyk,¹⁵ D. Toback,⁵¹ S. Tokar,¹² K. Tollefson,³³
T. Tomura,⁵³ D. Tonelli,¹⁵ S. Torre,¹⁷ D. Torretta,¹⁵ P. Totaro,^{ff,52} M. Trovato,^{dd,44} Y. Tu,⁴³
F. Ukegawa,⁵³ S. Uozumi,²⁵ A. Varganov,³² F. Vázquez,^{k,16} G. Velev,¹⁵ C. Vellidis,³ M. Vidal,²⁹
I. Vila,⁹ R. Vilar,⁹ M. Vogel,³⁵ G. Volpi,^{bb,44} P. Wagner,⁴³ R.L. Wagner,¹⁵ T. Wakisaka,³⁹
R. Wallny,⁸ S.M. Wang,¹ A. Warburton,³¹ D. Waters,²⁸ M. Weinberger,⁵¹ W.C. Wester III,¹⁵
B. Whitehouse,⁵⁴ D. Whiteson,^{c,43} A.B. Wicklund,² E. Wicklund,¹⁵ S. Wilbur,¹¹ F. Wick,²⁴
H.H. Williams,⁴³ J.S. Wilson,³⁷ P. Wilson,¹⁵ B.L. Winer,³⁷ P. Wittich,^{g,15} S. Wolbers,¹⁵ H. Wolfe,³⁷
T. Wright,³² X. Wu,¹⁸ Z. Wu,⁵ K. Yamamoto,³⁹ J. Yamaoka,¹⁴ T. Yang,¹⁵ U.K. Yang,^{p,11}
Y.C. Yang,²⁵ W.-M. Yao,²⁶ G.P. Yeh,¹⁵ K. Yi,^{m,15} J. Yoh,¹⁵ K. Yorita,⁵⁶ T. Yoshida,^{j,39}
G.B. Yu,¹⁴ I. Yu,²⁵ S.S. Yu,¹⁵ J.C. Yun,¹⁵ A. Zanetti,⁵² Y. Zeng,¹⁴ and S. Zucchelli,^{z6}

(CDF Collaboration[†])

¹*Institute of Physics, Academia Sinica, Taipei, Taiwan 11529, Republic of China*

²*Argonne National Laboratory, Argonne, Illinois 60439, USA*

³*University of Athens, 157 71 Athens, Greece*

⁴*Institut de Física d'Altes Energies, Universitat Autònoma de Barcelona, E-08193, Bellaterra (Barcelona), Spain*

⁵*Baylor University, Waco, Texas 76798, USA*

⁶*Istituto Nazionale di Fisica Nucleare Bologna,*

^z*University of Bologna, I-40127 Bologna, Italy*

⁷*University of California, Davis, Davis, California 95616, USA*

⁸*University of California, Los Angeles, Los Angeles, California 90024, USA*

⁹*Instituto de Física de Cantabria, CSIC-University of Cantabria, 39005 Santander, Spain*

¹⁰*Carnegie Mellon University, Pittsburgh, Pennsylvania 15213, USA*

¹¹*Enrico Fermi Institute, University of Chicago, Chicago, Illinois 60637, USA*

¹²*Comenius University, 842 48 Bratislava,*

- Slovakia; Institute of Experimental Physics, 040 01 Kosice, Slovakia
- ¹³Joint Institute for Nuclear Research, RU-141980 Dubna, Russia
- ¹⁴Duke University, Durham, North Carolina 27708, USA
- ¹⁵Fermi National Accelerator Laboratory, Batavia, Illinois 60510, USA
- ¹⁶University of Florida, Gainesville, Florida 32611, USA
- ¹⁷Laboratori Nazionali di Frascati, Istituto Nazionale di Fisica Nucleare, I-00044 Frascati, Italy
- ¹⁸University of Geneva, CH-1211 Geneva 4, Switzerland
- ¹⁹Glasgow University, Glasgow G12 8QQ, United Kingdom
- ²⁰Harvard University, Cambridge, Massachusetts 02138, USA
- ²¹Division of High Energy Physics, Department of Physics, University of Helsinki and Helsinki Institute of Physics, FIN-00014, Helsinki, Finland
- ²²University of Illinois, Urbana, Illinois 61801, USA
- ²³The Johns Hopkins University, Baltimore, Maryland 21218, USA
- ²⁴Institut für Experimentelle Kernphysik, Karlsruhe Institute of Technology, D-76131 Karlsruhe, Germany
- ²⁵Center for High Energy Physics: Kyungpook National University, Daegu 702-701, Korea; Seoul National University, Seoul 151-742, Korea; Sungkyunkwan University, Suwon 440-746, Korea; Korea Institute of Science and Technology Information, Daejeon 305-806, Korea; Chonnam National University, Gwangju 500-757, Korea; Chonbuk National University, Jeonju 561-756, Korea
- ²⁶Ernest Orlando Lawrence Berkeley National Laboratory, Berkeley, California 94720, USA
- ²⁷University of Liverpool, Liverpool L69 7ZE, United Kingdom
- ²⁸University College London, London WC1E 6BT, United Kingdom
- ²⁹Centro de Investigaciones Energeticas Medioambientales y Tecnologicas, E-28040 Madrid, Spain
- ³⁰Massachusetts Institute of Technology, Cambridge, Massachusetts 02139, USA
- ³¹Institute of Particle Physics: McGill University, Montréal, Québec, Canada H3A 2T8; Simon Fraser University, Burnaby, British Columbia, Canada V5A 1S6; University of Toronto, Toronto, Ontario, Canada M5S 1A7; and TRIUMF, Vancouver, British Columbia, Canada V6T 2A3
- ³²University of Michigan, Ann Arbor, Michigan 48109, USA
- ³³Michigan State University, East Lansing, Michigan 48824, USA
- ³⁴Institution for Theoretical and Experimental Physics, ITEP, Moscow 117259, Russia
- ³⁵University of New Mexico, Albuquerque, New Mexico 87131, USA
- ³⁶Northwestern University, Evanston, Illinois 60208, USA
- ³⁷The Ohio State University, Columbus, Ohio 43210, USA
- ³⁸Okayama University, Okayama 700-8530, Japan
- ³⁹Osaka City University, Osaka 588, Japan
- ⁴⁰University of Oxford, Oxford OX1 3RH, United Kingdom
- ⁴¹Istituto Nazionale di Fisica Nucleare, Sezione di Padova-Trento, ^{aa}University of Padova, I-35131 Padova, Italy
- ⁴²LPNHE, Universite Pierre et Marie Curie/IN2P3-CNRS, UMR7585, Paris, F-75252 France
- ⁴³University of Pennsylvania, Philadelphia, Pennsylvania 19104, USA
- ⁴⁴Istituto Nazionale di Fisica Nucleare Pisa, ^{bb}University of Pisa, ^{cc}University of Siena and ^{dd}Scuola Normale Superiore, I-56127 Pisa, Italy
- ⁴⁵University of Pittsburgh, Pittsburgh, Pennsylvania 15260, USA
- ⁴⁶Purdue University, West Lafayette, Indiana 47907, USA
- ⁴⁷University of Rochester, Rochester, New York 14627, USA
- ⁴⁸The Rockefeller University, New York, New York 10065, USA
- ⁴⁹Istituto Nazionale di Fisica Nucleare, Sezione di Roma 1, ^{ee}Sapienza Università di Roma, I-00185 Roma, Italy
- ⁵⁰Rutgers University, Piscataway, New Jersey 08855, USA
- ⁵¹Texas A&M University, College Station, Texas 77843, USA
- ⁵²Istituto Nazionale di Fisica Nucleare Trieste/Udine, I-34100 Trieste, ^{ff}University of Trieste/Udine, I-33100 Udine, Italy
- ⁵³University of Tsukuba, Tsukuba, Ibaraki 305, Japan
- ⁵⁴Tufts University, Medford, Massachusetts 02155, USA
- ⁵⁵University of Virginia, Charlottesville, VA 22906, USA
- ⁵⁶Waseda University, Tokyo 169, Japan

⁵⁷Wayne State University, Detroit, Michigan 48201, USA

⁵⁸University of Wisconsin, Madison, Wisconsin 53706, USA

⁵⁹Yale University, New Haven, Connecticut 06520, USA

The $t\bar{t}$ spin correlation at production is a fundamental prediction of QCD and a potentially incisive test of new physics coupled to top quarks. We measure the $t\bar{t}$ spin state in $p\bar{p}$ collisions at $\sqrt{s} = 1.96$ TeV using 1001 candidate events in the lepton plus jets decay channel reconstructed in the CDF II detector. In the helicity basis, for a top-quark mass of $172.5 \text{ GeV}/c^2$, we find a spin correlation coefficient $\kappa = 0.60 \pm 0.50$ (stat) ± 0.16 (syst), consistent with the QCD prediction, $\kappa \approx 0.40$.

PACS numbers: 12.38.Qk,14.65.Ha

In quark-pair production by the strong interaction, the quark spins are entangled according to the short distance dynamics of quantum chromodynamics (QCD) [1]. The spin state is observable in angular correlations among the quark decay products induced by the V-A nature of the weak interaction, but is typically destroyed by the depolarizing effects of hadronization before the decay can proceed. The top quark is an exception to this rule. Because of its large mass, the top-quark lifetime is shorter than the fragmentation timescale, cutting off the long distance QCD effects and transmitting the $t\bar{t}$ production configuration to the final state. Measurement of the $t\bar{t}$ spin configuration is a first look at a bare-quark pair at production. The measurement tests the

fundamental predictions of QCD [1–5] and could be a sensitive discriminant of new physics coupled to top quarks [6, 7]. For example, a $t\bar{t}$ resonance appearing as an excess in the $t\bar{t}$ invariant-mass spectrum can be verified as a Kaluza-Klein graviton through measurement of the spin correlation as described in Ref. [7].

Because final state charged leptons have the strongest correlation to the top-quark spin, the $t\bar{t}$ spin correlation is usually discussed in terms of the di-lepton final state $t\bar{t} \rightarrow (W^+b)(W^-\bar{b}) \rightarrow (\bar{\ell}\nu)(\ell'\bar{\nu}')b\bar{b}$ [4]. This mode suffers from a small branching ratio and poor definition of the top-quark kinematics due to the presence of two undetectable neutrinos. A previous measurement of the $t\bar{t}$ spin correlation was limited to a small sample of just six events in this mode [8].

We report on a new measurement of the $t\bar{t}$ spin correlation in $p\bar{p}$ collisions at 1.96 TeV with a data sample corresponding to an integrated luminosity of 4.3 fb^{-1} collected with the CDF II detector at the Fermilab Tevatron. We measure the spin correlation of pair-produced quarks for the first time in the lepton plus jets decay topology, $t\bar{t} \rightarrow (W^+b)(W^-\bar{b}) \rightarrow (u\bar{d}b)(\bar{\ell}\nu\bar{b})$ or $t\bar{t} \rightarrow (W^+b)(W^-\bar{b}) \rightarrow (\bar{\ell}\nu b)(\bar{u}d\bar{b})$ [9]. In this decay mode, we take advantage of a large branching ratio compared to the di-lepton channel and the well-constrained $t\bar{t}$ kinematics in the lepton plus jets final state with only one neutrino. The measurement relies critically on a new technique for identifying the final state down-type quark (d or s), which has the same spin-analyzing power as a charged lepton. We expect the spin correlation measurement to show the dominance of $t\bar{t}$ production via the $J=1$ $q\bar{q}$ annihilation channel that occurs in $\sim 85\%$ of $p\bar{p}$ collisions at the Tevatron [10].

We work in the helicity basis, where the spin-quantization axis is defined as the direction of motion of the t (or \bar{t}) quark in the $t\bar{t}$ rest frame.

*Deceased

[†]With visitors from ^aUniversity of Massachusetts Amherst, Amherst, Massachusetts 01003, ^bIstituto Nazionale di Fisica Nucleare, Sezione di Cagliari, 09042 Monserrato (Cagliari), Italy, ^cUniversity of California Irvine, Irvine, CA 92697, ^dUniversity of California Santa Barbara, Santa Barbara, CA 93106 ^eUniversity of California Santa Cruz, Santa Cruz, CA 95064, ^fCERN, CH-1211 Geneva, Switzerland, ^gCornell University, Ithaca, NY 14853, ^hUniversity of Cyprus, Nicosia CY-1678, Cyprus, ⁱUniversity College Dublin, Dublin 4, Ireland, ^jUniversity of Fukui, Fukui City, Fukui Prefecture, Japan 910-0017, ^kUniversidad Iberoamericana, Mexico D.F., Mexico, ^lIowa State University, Ames, IA 50011, ^mUniversity of Iowa, Iowa City, IA 52242, ⁿKinki University, Higashi-Osaka City, Japan 577-8502, ^oKansas State University, Manhattan, KS 66506, ^pUniversity of Manchester, Manchester M13 9PL, England, ^qQueen Mary, University of London, London, E1 4NS, England, ^rMuons, Inc., Batavia, IL 60510, ^sNagasaki Institute of Applied Science, Nagasaki, Japan, ^tNational Research Nuclear University, Moscow, Russia, ^uUniversity of Notre Dame, Notre Dame, IN 46556, ^vUniversidad de Oviedo, E-33007 Oviedo, Spain, ^wTexas Tech University, Lubbock, TX 79609, ^xUniversidad Tecnica Federico Santa Maria, 110v Valparaiso, Chile, ^yYarmouk University, Irbid 211-63, Jordan, ^{gg}On leave from J. Stefan Institute, Ljubljana, Slovenia,

A quark is called right-handed (t_R)/left-handed (t_L) if its spin is oriented along/opposite to its direction of motion. In the $t\bar{t}$ rest frame the quarks move back-to-back; thus the same-spin states with $J=1$ are those with opposite helicity: $\bar{t}_L t_R$ and $\bar{t}_R t_L$. Near the energy threshold for $t\bar{t}$ production, the opposite-helicity fraction is predicted in the standard model (SM) to be $\sim 67\%$ for $t\bar{t}$ production via $q\bar{q}$ annihilation, while for top quarks with large momenta compared to the top-quark mass, helicity is approximately conserved and this fraction rises to $\sim 100\%$ [1, 3]. Integrating over all top-quark momenta according to the parton distribution functions and adding the small ($\sim 15\%$) $J = 0$ contribution from gluon-gluon fusion processes, we expect to find an opposite-helicity fraction [1, 3]

$$F_{OH} = \frac{\sigma(\bar{t}_R t_L) + \sigma(\bar{t}_L t_R)}{\sigma(\bar{t}_R t_R) + \sigma(\bar{t}_L t_L) + \sigma(\bar{t}_R t_L) + \sigma(\bar{t}_L t_R)} \approx 0.70. \quad (1)$$

F_{OH} is simply related to the spin correlation coefficient κ that measures the fractional difference between the number of events in which the top-quark spins are aligned and the number of events in which they have opposite directions: $\kappa = 2F_{OH} - 1$. We thus expect $\kappa \approx 0.40$ [1, 3], while for uncorrelated spins, $\kappa = 0.0$ and $F_{OH} = 0.5$.

In top-quark decays in the SM the V-A couplings fix the angular distributions of the decay products according to the polarization of the parent top quark via

$$\frac{1}{\Gamma} \frac{d\Gamma}{d\cos\theta_i} = \frac{1}{2}(1 \pm A_i \cos\theta_i), \quad (2)$$

where the positive/negative sign is used for right-handed/left-handed quarks, and the helicity angle θ_i is defined as the angle between the spin-quantization direction and the momentum of the decay particle in the rest frame of its parent top quark. In the V-A weak decay, the spin-analyzing-power coefficient A_i is equal to $+1.0$ for the charged lepton or down-type quark, -0.41 for the bottom quark, and -0.31 for the neutrino or up-type quark, with the signs reversed for antitop-quark decays [3]. The $t\bar{t}$ spin correlation connects the daughter helicity angles on each side of the decay. The differential cross-section in these variables is

$$\frac{1}{\sigma} \frac{d^2\sigma}{d(\cos\theta_i)d(\cos\theta_j)} = \frac{1 + \kappa A_i A_j \cos\theta_i \cos\theta_j}{4}, \quad (3)$$

where i and j refer to top-quark and antitop-quark decay products respectively [3].

For each of the four possible $t\bar{t}$ helicity states, we create model templates for the distributions of $\cos\theta_l \cos\theta_d$ and $\cos\theta_l \cos\theta_b$, where the charged lepton l is a decay product from one top quark in the pair and the quarks d and b are decay products from the other quark. We then find the relative normalization of these model templates that gives the best fit to a two-dimensional distribution of these variables in the data. The model templates account for all acceptance effects and dilutions due to event reconstruction, so that the parton-level value of F_{OH} follows directly from the template fit to the data.

CDF II [11] is a general purpose, azimuthally and forward-backward symmetric detector. Charged-particle directions and momenta are measured with a silicon tracker [12] and a drift chamber [13] in a 1.4 T solenoidal magnetic field. Electromagnetic and hadronic calorimeters [14] are located beyond the solenoid and allow for jet and missing E_T reconstruction. Beyond the calorimeter, muon chambers [15] provide coverage for the pseudorapidity range $|\eta| \leq 1.0$. We use a cylindrical coordinate system with its origin at the center of the detector and the z-axis along the proton direction [16].

Lepton plus jets events are selected by requiring one electron or muon with transverse momentum of at least 20 GeV/ c and $|\eta| < 1.0$, missing transverse energy of at least 20 GeV, and four or more jets with transverse energy of at least 20 GeV and $|\eta| < 2.0$, at least one of which must be tagged as a b jet by the presence of a displaced secondary vertex [17]. This selection yields 1001 total candidate events, 224 of which have two tagged b jets.

Non- $t\bar{t}$ backgrounds are well-constrained by precision $t\bar{t}$ cross-section measurements [18], with a predicted total of 215 ± 48 background events. Non- $t\bar{t}$ models are checked against background-enriched sidebands with no tagged b jets and are found to give very good representations of the normalizations and kinematics in all variables, including lepton and jet energies and angular distributions.

The helicity angles are determined in a complete reconstruction of the $t\bar{t}$ kinematics in $t\bar{t} \rightarrow (Wb)(Wb) \rightarrow (\ell\nu b)(udb)$, where we constrain $M(\ell\nu) = M(ud) = 80.4 \text{ GeV}/c^2$, the mass of the W boson, and $M(\ell\nu b) = M(udb) = 172.5 \text{ GeV}/c^2$, the top-quark mass, and require any tagged b jets to be identified with b partons. The constraints were chosen to be close to the world averages in Ref. [19]. Each of the 24 possible jet-to-parton assignments is evaluated using a χ^2 comparison to the $t\bar{t}$ hypothesis with the above constraints, and we choose the assignment with the lowest χ^2 value [20]. This procedure correctly assigns all jets to the corresponding partons in approximately 37% of events. All effects of angular acceptance and jet reconstruction and mis-assignment are fully modeled by our simulated samples.

Down-type-quark identification relies on the V-A decay correlation that tends to send the down-type quark in the direction opposite that of the hadronically decaying W boson in the top-quark rest frame. We therefore assign the down-type quark as the jet that, in the W boson rest frame, is closest to the bottom jet identified as coming from the same top quark as the W boson [3]. Simulation studies show that this algorithm correctly identifies the down-type quark 60% of the time.

The same-helicity and opposite-helicity model templates are created with a customized version of the HERWIG event generator [21] that implements the angular distribution of Eq. 2 for the charged lepton or down-type quark, with a tunable choice of right- or left-handed top quarks, and preserves all the other expected spin correlations [22]. We create four different simulated samples, corresponding to the four possible top-quark-pair helicity states: $\bar{t}_L t_R$, $\bar{t}_R t_L$, $\bar{t}_L t_L$, and $\bar{t}_R t_R$. QCD interactions respect both the parity symmetry (P) and the combined symmetry of parity and charge conjugation (CP). Because CP transforms $\bar{t}_R t_R \rightarrow t_L \bar{t}_L$, we can define the same-helicity (SH) model template shape to be the symmetric sum of $\sigma(\bar{t}_R t_R) + \sigma(t_L \bar{t}_L)$. Since P transforms $\bar{t}_R t_L \rightarrow \bar{t}_L t_R$, we let the opposite-helicity (OH) model template shape be the symmetric sum of $\sigma(\bar{t}_R t_L) + \sigma(\bar{t}_L t_R)$.

Figure 1 compares the SH and OH model templates after detector simulation, event selection, and reconstruction in the two distributions that we use for the measurement, $\cos\theta_l \cos\theta_d$ and

$\cos\theta_l \cos\theta_b$. Our sensitivity results from the SH model template being shifted towards negative values of $\cos\theta_l \cos\theta_d$, while the OH model template is shifted towards positive values, with the opposite shifts occurring in the $\cos\theta_l \cos\theta_b$ distribution.

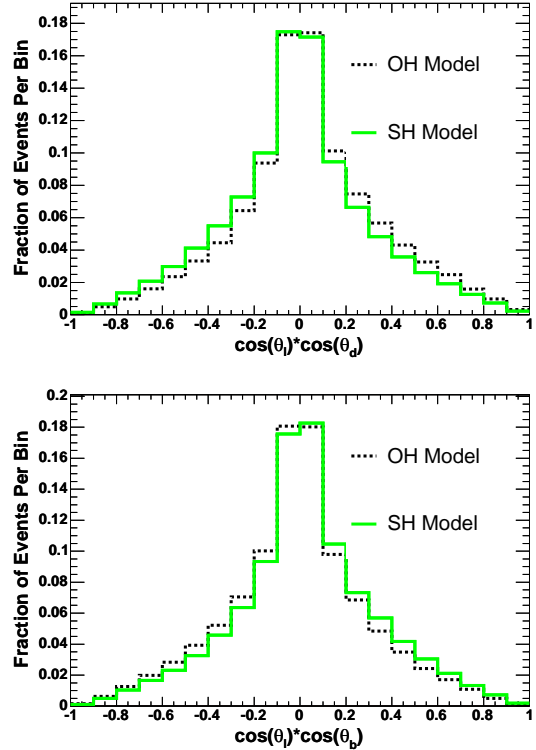


FIG. 1: Distributions of the $\cos\theta_l \cos\theta_d$ and $\cos\theta_l \cos\theta_b$ variables, after detector simulation, event selection, and reconstruction, in our same-helicity and opposite-helicity simulated $t\bar{t}$ samples.

We perform our measurement using a binned likelihood fit to find the relative normalization of these model templates that gives the best simultaneous representation of $\cos\theta_l \cos\theta_d$ and $\cos\theta_l \cos\theta_b$ in our data. The background normalization is constrained to be close to the predicted value, with a Gaussian uncertainty, but the same-helicity fraction F_{SH} and opposite-helicity fraction F_{OH} are allowed to float freely. We do not require that F_{SH} and F_{OH} be constrained to physical values between 0 and 1, but we do require $F_{SH} + F_{OH} = 1$. The fit runs over all bins in a two-dimensional distribution of $\cos\theta_l \cos\theta_d$ vs. $\cos\theta_l \cos\theta_b$. The expected statistical uncertainty for F_{OH} is approximately 0.23, corresponding to

an uncertainty for κ of 0.46, and is independent of the actual value of F_{OH} and κ .

TABLE I: Systematic Uncertainties on F_{OH}

Systematic	Uncertainty
Generator dependence	0.060
JES	0.042
ISR/FSR	0.030
Background shape	0.023
Color reconnection	0.009
PDF	0.007
Parton shower	0.006
Background size	0.002
Total uncertainty	0.083

Additional contributions to the uncertainty result from incomplete knowledge of the background size and shape, of the exact detector response, and of the parton distribution functions (PDF), and are estimated by performing the measurement in simulated samples with reasonable variations in the model assumptions. These systematic uncertainties are shown in Table I. The largest uncertainty, generator dependence, results from small biases seen when testing with simulated samples created using a range of generators, including HERWIG [21], PYTHIA [23], ALPGEN [24], and MADEVENT [25]. Other significant contributions come from the uncertainty of the jet energy scale (JES) during event reconstruction and uncertainty in the amount of initial and final state radiation (ISR/FSR) in our observed $t\bar{t}$ events. The small variation of F_{OH} with the assumed value of the top-quark mass is not included in our systematic uncertainty; our measurement assumes a mass of $172.5 \text{ GeV}/c^2$ for the top quark.

The final result of our fit to the two-dimensional distribution $\cos\theta_l \cos\theta_d$ vs. $\cos\theta_l \cos\theta_b$ is shown in Fig. 2. This figure shows one-dimensional distributions of both variables, with our data being compared to the sum of the background model, same-helicity model, and opposite-helicity model, with the model normalizations determined by our fit result. Assuming the top-quark mass is $172.5 \text{ GeV}/c^2$, we find an opposite-helicity fraction of

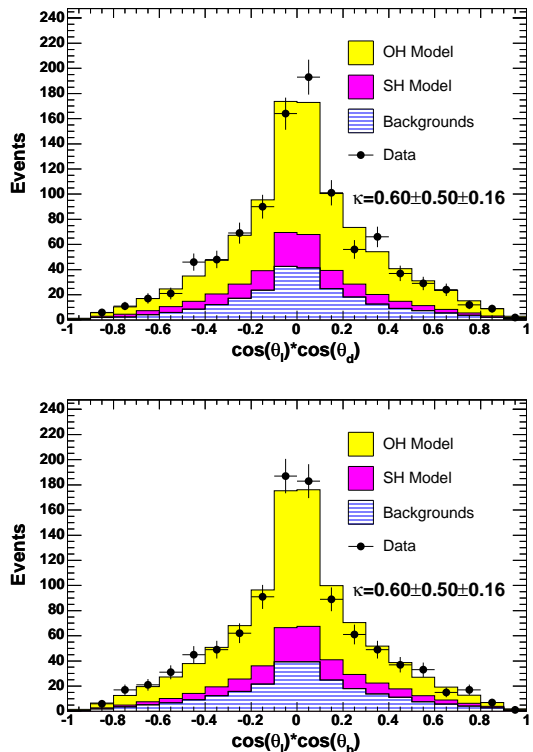


FIG. 2: Distribution of the $\cos\theta_l \cos\theta_d$ and $\cos\theta_l \cos\theta_b$ variables in data compared to the sum of our background model, the same-helicity model template, and the opposite-helicity model template. The relative normalizations of the model distributions are determined by our fit result.

$$F_{OH} = 0.80 \pm 0.25 \text{ (stat)} \pm 0.08 \text{ (syst)} .$$

Converting this to the spin correlation coefficient, using $\kappa = 2F_{OH} - 1$, yields

$$\kappa = 0.60 \pm 0.50 \text{ (stat)} \pm 0.16 \text{ (syst)} .$$

This first measurement of the top-quark pair spin correlation in the lepton plus jets decay channel agrees well with the theoretical prediction of $\kappa \approx 0.40$ [1, 3], although the statistical uncertainty is still large. If the Tevatron dataset reaches 15 fb^{-1} before the end of the Tevatron lifetime, the expected statistical uncertainty on κ would be reduced to 0.26. This technique can thus be applied in future measurements with larger datasets collected at the Tevatron and

LHC to constrain the $t\bar{t}$ production spin structure or to connect with other anomalies that may show up in the reconstructable $t\bar{t}$ kinematics of the lepton plus jet sample.

We thank the Fermilab staff and the technical staffs of the participating institutions for their vital contributions. This work was supported by the U.S. Department of Energy and National Science Foundation; the Italian Istituto Nazionale di Fisica Nucleare; the Ministry of Education, Culture, Sports, Science and Technology of Japan; the Natural Sciences and Engineering Research Council of Canada; the National Science Council of the Republic of China; the Swiss National Science Foundation; the A.P. Sloan Foundation; the Bundesministerium für Bildung und Forschung, Germany; the World Class University Program, the National Research Foundation of Korea; the Science and Technology Facilities Council and the Royal Society, UK; the Institut National de Physique Nucleaire et Physique des Particules/CNRS; the Russian Foundation for Basic Research; the Ministerio de Ciencia e Innovación, and Programa Consolider-Ingenio 2010, Spain; the Slovak R&D Agency; and the Academy of Finland.

-
- [1] T. Steltzer and S. Willenbrock, Phys. Lett. B **374**, 169 (1996); A. Brandenburg, *ibid.* **388**, 626 (1996).
- [2] V.D. Barger, J. Ohnemus, and R.J.N. Phillips, Int. J. Mod. Phys. **A4**, 671, (1989); D. Chang, S.C. Lee, and A. Soumarokov, Phys. Rev. Lett. **77**, 1218 (1996).
- [3] G. Mahlon and S. Parke, Phys. Rev. D **53**, 4886 (1996); Phys. Lett. B **411**, 173 (1997).
- [4] T. Arens and L.M. Sehgal, Phys. Lett. B **302**, 501 (1993).
- [5] W. Bernreuther *et al.*, Phys. Rev. Lett. **87**, 242002 (2001); Nucl. Phys. **B690**, 81 (2004); P. Uwer, Phys. Lett. B **609**, 271 (2005); G. Mahlon and S. Parke, Phys. Rev. D **81**, 074024, 2010.
- [6] G.L. Kane, G.A. Ladinsky, and C.P. Yuan, Phys. Rev. D **45**, 124 (1992); K. Chung, *ibid.* **55**, 4430 (1997); B. Holdom and T. Torma, *ibid.* **60**, 114010 (1999); M. Arai *et al.*, *ibid.* **70**, 115015 (2004); Acta. Phys. Pol. B **40**, 93 (2009); M. Arai, N. Okada, and K. Smolek, Phys. Rev. D **79**, 074019 (2009); J.Y. Liu, Z.G. Si, and C.X. Yue, *ibid.* **81**, 015011 (2010).
- [7] M. Arai *et al.*, Phys. Rev. D **75**, 095008 (2007).
- [8] B. Abbott *et al.* (D0 Collaboration), Phys. Rev. Lett. **85**, 256 (2000).
- [9] Throughout this Letter, when we refer to a u quark, we mean either a u or c quark, and similarly, a d quark refers to either a d or s quark. Additionally, unless necessary, we do not differentiate between a particle and its antiparticle, so the inclusion of the charge-conjugate state should be assumed.
- [10] N. Kidonakis and R. Vogt, Phys. Rev. D **68**, 114014 (2003).
- [11] A. Abulencia *et al.* (CDF Collaboration), J. Phys. G Nucl. Part. Phys. **34**, (2007).
- [12] C. Hill *et al.* (CDF Collaboration), Nucl. Instrum. Methods, **A530**, 1 (2004); A. Sill *et al.* (CDF Collaboration), *ibid.*, **A447**, 1 (2000); A. Affoldner *et al.* (CDF Collaboration), *ibid.*, **A453**, 84 (2000).
- [13] T. Affoldner *et al.* (CDF Collaboration), Nucl. Instrum. Methods, **A526**, 249 (2004).
- [14] L. Balka *et al.* (CDF Collaboration), Nucl. Instrum. Methods, **A267**, 272 (1988); S. Bertolucci *et al.* (CDF Collaboration), Nucl. Instrum. Methods, **A267**, 301 (1988).
- [15] G. Ascoli *et al.* (CDF Collaboration), Nucl. Instrum. Methods, **A268**, 33 (1998).
- [16] In CDF's cylindrical coordinate system, the transverse momentum is defined as $p_T = p \sin \theta$, where θ is the polar angle measured from the proton direction (z-axis). Similarly, the transverse energy is defined as $E_T = E \sin \theta$. The missing transverse energy is defined by $\cancel{E}_T = |\vec{\cancel{E}}_T| = |-\sum_i E_T^i \hat{n}_i|$ where \hat{n}_i is a unit vector perpendicular to the beam axis and pointing to the i^{th} calorimeter tower. The pseudorapidity is defined as $\eta = -\ln \tan(\theta/2)$.
- [17] T. Affolder *et al.* (CDF Collaboration), Phys. Rev. D **64**, 032002 (2001).
- [18] T. Aaltonen *et al.* (CDF Collaboration), Phys. Rev. Lett. **105**, 012001 (2010).
- [19] K. Nakamura *et al.* (Particle Data Group), J. Phys. G **37**, 075021 (2010).
- [20] A. Abulencia *et al.* (CDF Collaboration), Phys. Rev. D **73**, 032003 (2006).
- [21] G. Corcella *et al.*, J. High Energy Phys. **01** (2001) 010.
- [22] E. Guillian, Ph.D. thesis, University of Michigan, FERMILAB-THESIS-1999-51, 1999.
- [23] T. Sjostrand, L. Lonnblad, and S. Mrenna, Comput. Phys. Commun. **101**, 232 (1997).
- [24] M. Mangano *et al.*, J. High Energy Phys. **07** (2003) 001.
- [25] F. Maltoni and T. Stelzer, J. High Energy Phys. **02** (2003) 027.